MPRA
Munich Personal RePEc Archive

Correction Power factor through FACTS devices

yazdi, saber and safa, Reza and abdi, mahsa

2022

Online at https://mpra.ub.uni-muenchen.de/116416/
MPRA Paper No. 116416, posted 20 Feb 2023 09:28 UTC

Correction Power factor through FACTS devices

Saber yazdi, Reza safa, Mahsa abdi

Abstract

Industrial power plants are able to generate electricity with appropriate quality and power factor using Instrumentation.

These plants use traditional methods to avoid the heavy compensation that may be imposed on them, and also use capacitive banks or newer solutions such as SVC and STATCOM, which are too expensive to improve power factor. They also use separate active filters to reduce current harmonics. This paper proposes that dynamic capacitors that are based on inverters used as a capacitive dynamic controller with an active harmonic filter make this system cost less than SVC and STATCOM.

Introduction

Power factor correction is one of the best ways to focus on investing and reducing energy costs, which funds will be returned in a short amount of time [1-2]. Advances in recent years have increased the reliability and capacity of the compensation system. In many cases, system design and estimation of dimensions has become more difficult due to the annual increase in harmonics in low and medium pressure networks [3-5]. Power converters, motor controllers, fixed frequency converters, televisions and computers inject harmonic currents into networks and these harmonics may be amplified by network impedance and capacitors [6-8].

Compensators such as SVC and STATCOM are used for power of 20-100 MVAR and at a voltage level of 350 kV. Compensators such as SVCs are controlled by thyristors, reactors and fixed capacitors. These compensators have been in use for 30 years. Also, STATCOM, which is based on DC / AC inverter for reactive power control, has been used commercially for about 3 years. Active filters on the market have less penetration in the market due to low reliability and high relative cost [7].

The conventional solution for modifying the power factor using a capacitive bank can be changed with a shunt. Its single-line diagram is shown in Figure 1-A. This capacitor bank from 6 to 3 electromechanical switches that inject reactive power into the circuit in the form of step changes according to Figure 1-B to correct the power factor. In order to prevent harmonic current, an active filter with high switching frequency and an inverter with DC / AC bandwidth control should be used. In fact, this system has a high cost and a lot of complexity [9].

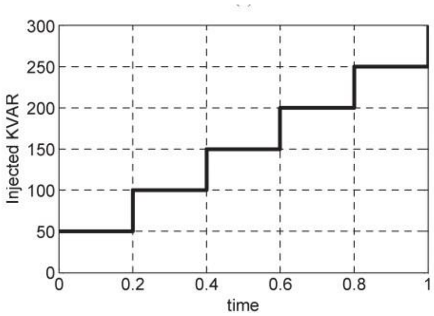

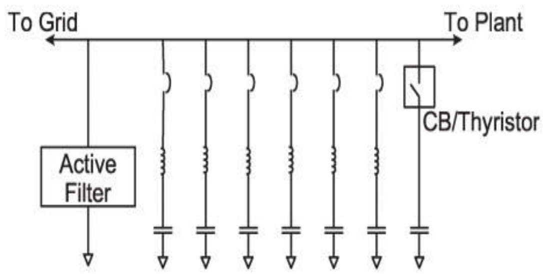

Dynamic capacitor:

The dynamic capacitor consists of a small AC and LC chopper (L_{f1}, L_{f2}, C_f) and capacitor C, which is used to suppress the harmonics caused by the switches and to modify the power factor.

The structure of the D-CAP is shown in Figure 2-A. This dynamic var compensator has the same performance as STATCOM. [4]

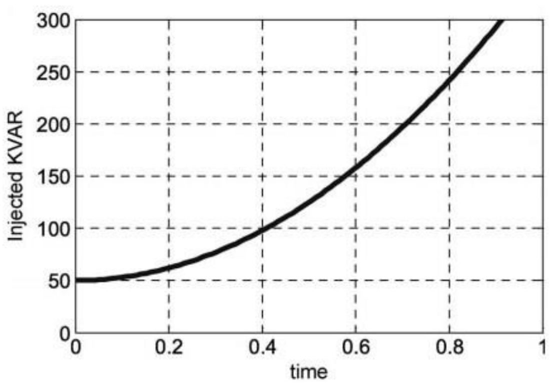

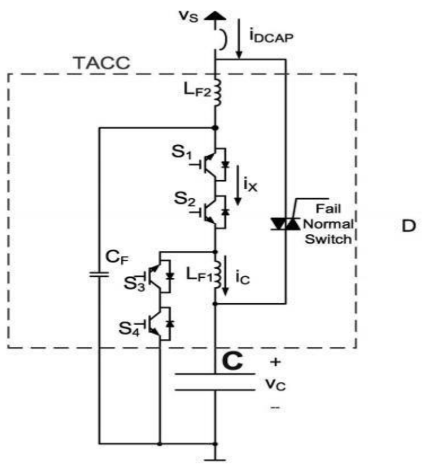

If the AC chopper is modulated with the cycle D = k_0 at high frequency f, the equations V_c and I_x are obtained from the following equation:

$$V_c = K_0 V_m Sin(wt) \quad (1)$$

$$I_x = \frac{K_0^2 V_m}{X_c} Cos(wt) \quad (2)$$

In fact, the D-Cap works like a dynamically variable capacitor. It is like a thyristor-controlled reactor (TCR) in which the effective amount of inductance is controlled. Unlike TCR, however, it does not produce low-frequency D-Cap harmonics, and can control it quickly. In addition, each phase operates independently of the other two phases [3].

When the task factor equal one, the maximum reactive power is transmitted from the capacitor to the network (C + C_f), and when the task factor D equal zero, the minimum reactive power is injected into the system.

The effective value of Var can be controlled by sub-cycle response time by controlling the task factor. Therefore, the amount of capacitor C is selected based on the amount of reactive power required to produce the appropriate power quality during the day. The values of L_{f1}, L_{f2}, C_f affect the switching frequency, which is used to reduce the harmonic effect of switching [4,5].

Active filter control strategy:

The control strategy of active filters depends not only on the purpose of compensation and the amount of nominal capacity of the filter, but also on the characteristics of the filters in transient and permanent states [9-11].

There are two types of control strategies for active filters: one is the p-q instantaneous power theory in the time domain only for three-phase circuits and the other is Fourier analysis in the frequency domain.

Most active filters today use instantaneous reactive power theory as a control strategy.

In this paper, the active filters work based on the interaction of the switches. These switches are controlled by pulse width modulation (PWM) [6]. The working cycle of the switches is obtained from the following equation [12-14].

$$D(t) = \frac{V_0^*}{V_m Sin(wt)} \tag{3}$$

$$V_0^* = V_1 Sin(wt + \varphi_1) + V_3 Sin(wt + \varphi_3) + V_5 Sin(wt + \varphi_5) + \cdots \tag{4}$$

$$D(t) = K_0 + K_2 Sin(wt + \varphi_2) + K_4 Sin(wt + \varphi_4) + \cdots \tag{5}$$

The mathematical equation of the current injected by the D-Cap when the switches are disconnected and connected to the duty cycle D (t) are:

$$I_{D-Cap}(t) = D(t). C \frac{d}{dt}\big(D(t). V_s(t)\big) = I_w(t) + I_{3w}(t) + I_{5w}(t) + I_{7w}(t) \tag{6}$$

$$I_w(t) = \frac{1}{2} V_m wC[2K_0^2 Cos(wt) + K_2^2 Cos(wt) + K_4^2 Cos(wt)] \tag{7}$$

$$I_{3w}(t) = \frac{1}{4} V_m wC[8K_0K_2 Sin(3wt + \varphi_2) + K_2^2 Cos(3wt + 2\varphi_2) - 4K_0K_2 Sin(3wt + \varphi_4)]$$

$$+4K_4K_2 Cos(3wt - \varphi_2 + \varphi_4)] \tag{8}$$

$$I_{5w}(t) = \frac{1}{4} V_m wC[12K_0K_2 Sin(5wt + \varphi_4) + 3K_2^2 Cos(5wt + 2\varphi_4)]$$

$$+4K_4K_2 Cos(5wt - \varphi_2 + \varphi_4) \tag{9}$$

$$I_{7w}(t) = \frac{1}{4} V_m wC[-8K_4K_2 Sin(7wt + \varphi_2 + \varphi_4) + 3K_4^2 Cos(7wt + 2\varphi_4)] \tag{10}$$

simulation:

This simulation is performed with MATLAB software. The general model of the system is shown in Figure 0, where a nonlinear load consisting of a three-phase rectifier diode is connected in parallel to a set of loads. Three single-phase D-Caps connected to one line from one side and all three from the other side, which have been used to reduce the harmonic of the network and modify the power factor.

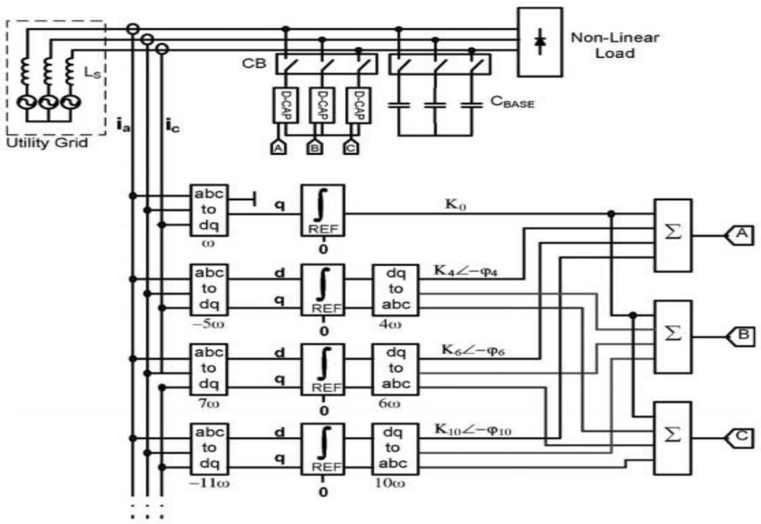

In this simulation, instantaneous power theory is used to control D-Caps, which includes two general control loops. One loop is used to reduce the harmonic due to switching and the other loop is used to modify the power factor. Each harmonic control loop is used to remove a specific frequency harmonic The power factor correction loop in the main frequency first uses the abc to dq conversion, which is the same as the **direct-quadrature-zero**. Then we set the component q to zero. The integral output is then obtained from it to obtain a constant value that determines how much reactive power should be injected into the system.

Each of the harmonic current control loops similarly converts abc to dq. After integration, output converts to abc again. The output of the loops is concluded together. Where the function D (t) is obtained. The function D (t) is then modulated In Figure 4, we notice the control loops of power factor correction and harmonic reduction of 5 and 7.

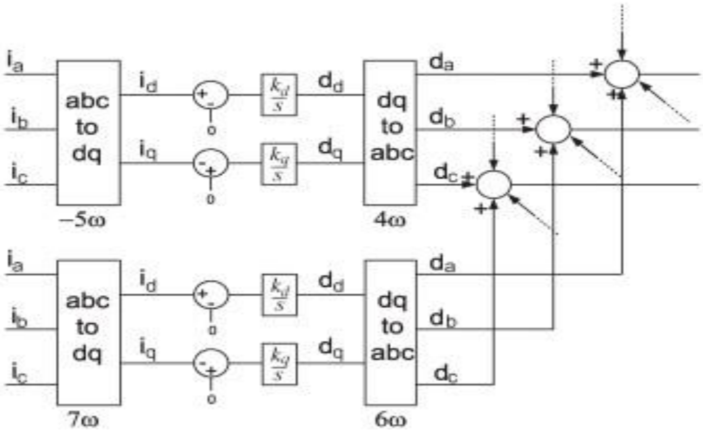

An example of a single-phase designed system is shown below.

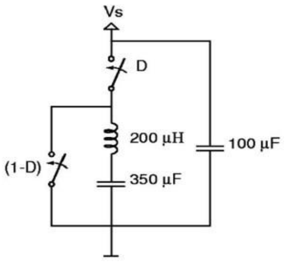

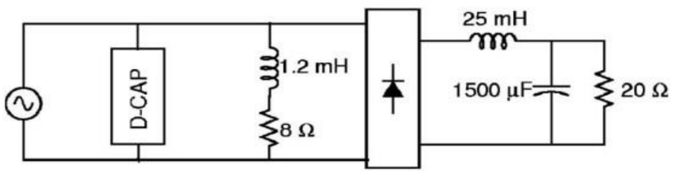

Simulation results:

Matlab software has been used to simulate the system. The studied system is shown in Figure (3). To analyze the system and study its actions, the system is first simulated without the presence of D-Cap and the waveforms are shown.

The simulation results show that the current is out of sinusoidal state due to the nonlinear load at the end of the line. Due to the harmonic analysis, we conclude that the line has harmonics 5, 7, 00 and 00(The value of each harmonica is given as a percentage of the original frequency in Appendix 0) Which is THD = 31.44%. After connecting the D-Cap, the following results are obtained by controlling the reactive power injected into the line by the switches.

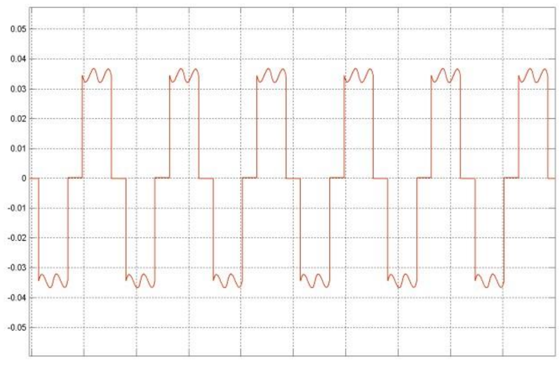

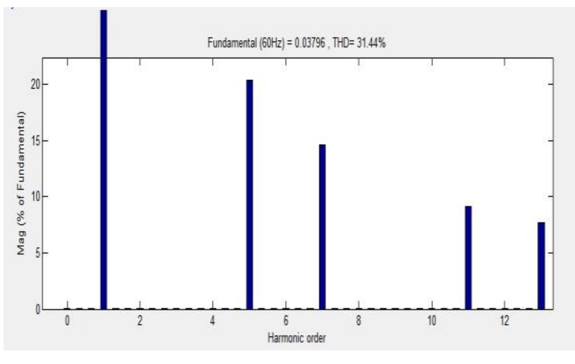

The simulation results show that the line current becomes sinusoidal after connecting D-Cap.

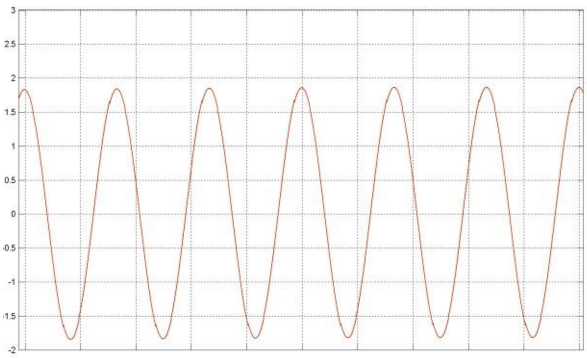

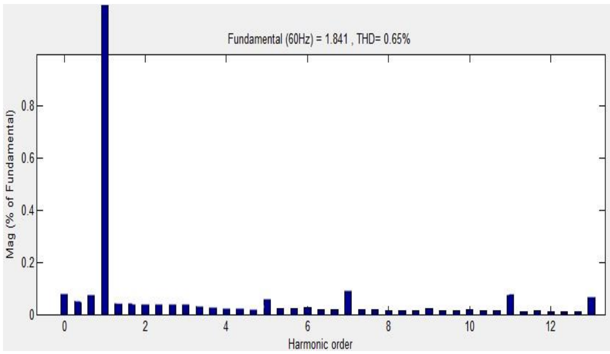

Due to harmonic analysis we conclude that the harmonic values of 5, 7, 00 and 00 have decreased.

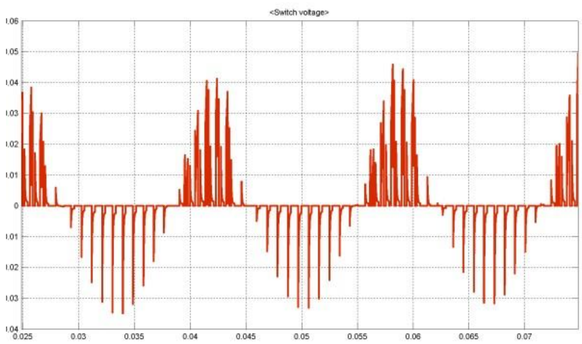

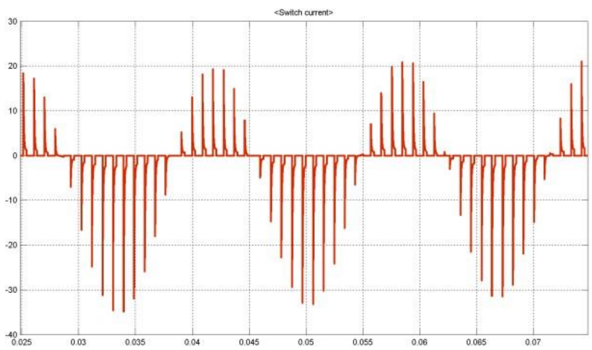

(The value of each harmonica is given as a percentage of the main frequency in Appendix 0) which is THD = 0.65%

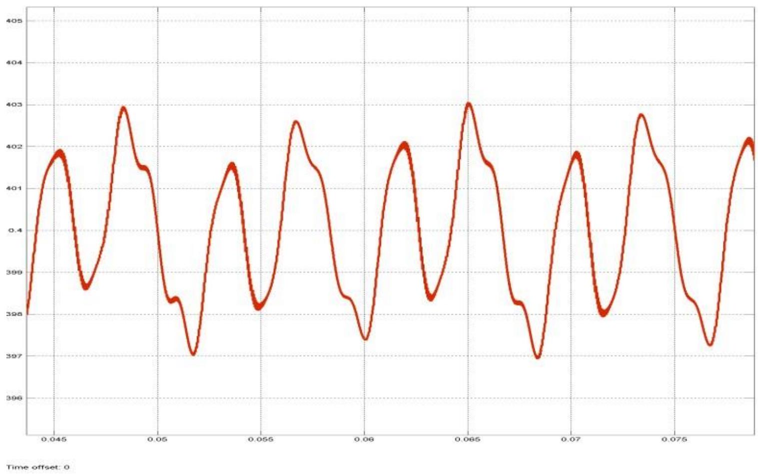

( )

Harmonics with and W/O D-cap

Total Harmonic Distortion (THD) = 31.44%

Maximum harmonic frequency
used for THD calculation = 249900.00 Hz (4165th harmonic)

0 Hz	(DC):	0.00%	90.0°
20 Hz		0.02%	252.6°
40 Hz		0.00%	155.6°
60 Hz	(Fnd):	100.00%	35.5°
80 Hz		0.00%	265.2°
100 Hz		0.01%	2.5°
120 Hz	(h2):	0.00%	-34.9°
140 Hz		0.01%	-33.8°
160 Hz		0.00%	10.3°
180 Hz	(h3):	0.00%	-70.7°
200 Hz		0.00%	20.8°
220 Hz		0.01%	252.8°
240 Hz	(h4):	0.00%	68.0°
260 Hz		0.01%	216.4°
280 Hz		0.00%	114.5°
300 Hz	(h5):	20.35%	-10.6°
320 Hz		0.00%	226.5°
340 Hz		0.02%	-35.6°
360 Hz	(h6):	0.00%	223.3°
380 Hz		0.02%	-71.6°
400 Hz		0.00%	225.4°
420 Hz	(h7):	14.58%	83.7°
440 Hz		0.00%	-51.4°
460 Hz		0.01%	36.2°
480 Hz	(h8):	0.00%	-0.1°
500 Hz		0.01%	0.3°
520 Hz		0.00%	22.9°
540 Hz	(h9):	0.00%	-35.7°
560 Hz		0.00%	32.5°
580 Hz		0.01%	-71.6°
600 Hz	(h10):	0.00%	104.5°
620 Hz		0.01%	252.2°
640 Hz		0.00%	160.2°
660 Hz	(h11):	9.09%	36.2°
680 Hz		0.00%	267.7°
700 Hz		0.02%	0.2°
720 Hz	(h12):	0.00%	258.8°
740 Hz		0.02%	-35.8°
760 Hz		0.00%	266.4°
780 Hz	(h13):	7.72%	112.8°

Total Harmonic Distortion (THD) = 0.65%

Maximum harmonic frequency
used for THD calculation = 249900.00 Hz (4165th harmonic)

0 Hz	(DC):	0.91%	270.0°
20 Hz		0.44%	177.8°
40 Hz		0.20%	176.3°
60 Hz	(Fnd):	100.00%	-50.8°
80 Hz		0.10%	179.0°
100 Hz		0.08%	184.1°
120 Hz	(h2):	0.07%	177.2°
140 Hz		0.05%	179.5°
160 Hz		0.05%	180.5°
180 Hz	(h3):	0.04%	177.0°
200 Hz		0.04%	180.0°
220 Hz		0.04%	183.9°
240 Hz	(h4):	0.03%	185.0°
260 Hz		0.03%	185.2°
280 Hz		0.03%	183.0°
300 Hz	(h5):	0.39%	-11.4°
320 Hz		0.02%	181.6°
340 Hz		0.02%	179.6°
360 Hz	(h6):	0.03%	178.0°
380 Hz		0.02%	179.4°
400 Hz		0.02%	178.7°
420 Hz	(h7):	0.31%	87.7°
440 Hz		0.02%	177.6°
460 Hz		0.02%	171.3°
480 Hz	(h8):	0.01%	187.2°
500 Hz		0.02%	175.9°
520 Hz		0.01%	181.4°
540 Hz	(h9):	0.02%	175.1°
560 Hz		0.01%	178.7°
580 Hz		0.01%	178.9°
600 Hz	(h10):	0.02%	188.5°
620 Hz		0.01%	177.5°
640 Hz		0.01%	180.9°
660 Hz	(h11):	0.18%	38.3°
680 Hz		0.01%	179.2°
700 Hz		0.01%	175.1°
720 Hz	(h12):	0.01%	177.5°
740 Hz		0.01%	187.5°
760 Hz		0.01%	185.0°
780 Hz	(h13):	0.16%	116.5°

Conclusion:

In this paper, we present an integrated method for reducing harmonics and modifying the power factor. This method, known as dynamic capacitors, is based on inverters as a capacitive dynamic controller with an integrated harmonic filter to be used at the expense of this system. Less than SVC and statcom due to the shown waveforms obtained from two modes with D-Cap and without D-Cap, it was shown that this new method reduces THD.

Appendix 0 The value of each of the harmonics as a percentage of the main frequency in the state without D - Cap

The value of each harmonic as a percentage of the main frequency in the case with D-Cap

* The reason for using inductors and capacitors in the following circuit:

The converter consists of a small LC chopper ($_1Lf_2$ L_f, C_f) used to suppress switching harmonics and a capacitor C to modify the power factor.

The VQS method is a method that controls the voltage across the axis and can control the harmonics and the phase and amplitude of the output voltage.

Assume that V_{in} is the input voltage, which we consider on the d-axis, and V_o is the optimum output voltage, which is shifted by φ relative to the input voltage. The output voltage is obtained from the sum of the two components of the q and d axes. Figure 1 shows the equivalent circuit of the chopper when the controller is with EHM, and Figure 2 shows the input voltage and the voltage of the q axis with the main frequency and three times the main frequency, Figure 2 shows the input and output voltages that are harmonically affected.

In this method we have:

Due to physical limitations

In order to obtain the desired output voltage, 0 = θ must be obtained

If the control variable is V_{qo}, if it is $\varphi_3 = \frac{}{2}$, then it is the minimum level of the third harmonic that must be injected into the system to achieve the desired control. This can be calculated by the function.

It is simplified to the following form

* A comparison of the D-CAP topology in each phase with the capacitor bank and VSI inverter topology is shown in the figure below.

VSI is a reactive power compensator with only a relatively small capacitor on the dc side. The following figure shows the single-phase diagram of a VSI and the input phase diagram of VSI voltages and line voltages.

As can be seen, the VSI is connected to the system by an inductor, which is used to filter out additional harmonics. This inductor shows a large impedance against high frequency harmonics and prevents the flow of those harmonics.

As shown in the fuzzy diagram of the pre-phase mode, the output voltage of the VSI is less than the mains voltage, the reactive power is absorbed by the VSI; The network is injected.

References:

[1] Bindal, Ranjit Kumar. "A Review of Benefits of FACTS Devices in Power system." *International Journal of Engineering and Advanced Technology (IJEAT)* 3, no. 4 (2014): 105-108.

[2] Y. Muhammad, R. Khan, F. Ullah, and Y. He, “Solution of optimal reactive power dispatch with FACTS devices”: a survey. *Energy Reports*, *6*, pp.2211-2229.

[3] A. Yousefi, H. Zareipour, “Congestion management using demand response and FACTS devices”. *International Journal of Electrical Power & Energy Systems*, *37*(1), pp.78-85.

[4] E. Ghahremani, and I. Kamwa, “Optimal placement of multiple-type FACTS devices to maximize power system loadability using a generic graphical user interface”. *IEEE transactions on power systems*, *28*(2), pp.764-778.

[5] Yao, W., Jiang, L., Wen, J., Wu, Q.H. and Cheng, S., 2013. Wide-area damping controller of FACTS devices for inter-area oscillations considering communication time delays. IEEE Transactions on Power Systems, 29(1), pp.318-329.

[6] M. Hayerikhiyavi and A. Dimitrovski, "Impact of Different Types of DC Bias Sources on the Effective Impedance of a CVSR," 2022 IEEE Kansas Power and Energy Conference (KPEC), 2022, pp. 1-6, doi: 10.1109/KPEC54747.2022.9814785.

[7] M. Hayerikhiyavi and A. Dimitrovski, "Improved Gyrator-Capacitor Modeling of Magnetic Circuits with Inclusion of Magnetic Hysteresis," 2022 IEEE/PES Transmission and Distribution Conference and Exposition (T&D), 2022, pp. 1-5, doi: 10.1109/TD43745.2022.9816976.

[8] M. Hayerikhiyavi and A. Dimitrovski, "Gyrator-Capacitor Modeling of A Continuously Variable Series Reactor in Different Operating Modes," 2021 IEEE Kansas Power and Energy Conference (KPEC), 2021, pp. 1-5, doi: 10.1109/KPEC51835.2021.9446236

[9] S. Chirantan, and R. Jena, R, “Enhancement of power profiles by various FACTS devices in power system”. In *2017 2nd International Conference on Communication and Electronics Systems (ICCES)* (pp. 896-901).

[10] A. Kumar, and C. Sekhar, “Congestion management with FACTS devices in deregulated electricity markets ensuring loadability limit”. *International Journal of Electrical Power & Energy Systems*, *46*, pp.258-273.

[11] A.R. Jordehi, “Optimal allocation of FACTS devices for static security enhancement in power systems via imperialistic competitive algorithm (ICA)”. *Applied Soft Computing*, *48*, pp.317-328.

[12] V. Frolov, P.G. Thakurta, S. Backhaus, J. Bialek, and M. Chertkov, “Operations-and uncertainty-aware installation of FACTS devices in a large transmission system”. *IEEE transactions on control of network systems*, *6*(3), pp.961-970.

[13] S. Bagchi, R. Bhaduri, and S. Banerjee, “Analysis of power transfer capability of a long transmission line using FACTS devices”. In *2015 International Conference on Advances in Computing, Communications and Informatics (ICACCI)* (pp. 601-606).

[14] W. Aslam, Y. Xu, A. Siddique, and F.M Albatsh, “Implementation of series facts devices SSSC and TCSC to improve power system stability” In *2018 13th IEEE Conference on Industrial Electronics and Applications (ICIEA)* (pp. 2291-2297).